



OPEN Flavonoids from *Polygonum hydropiper* L. regulate PCV2-induced oxidative stress of RAW264.7 cells via Pi3k/AKT and Nrf2/HO-1 signaling pathways

Qi Chen¹, Qihua Wang¹, Yi Zhao¹, Xiaodong Xie¹, HeYu Feng¹, Yingyi Wei¹, Meiling Yu¹, Xianhui Pan^{1,2}✉ & Tingjun Hu¹✉

Flavonoid n-butanol (FNB) possess diverse pharmacological properties. This study aimed to explore the mechanism of FNB in regulating oxidative response in PCV2-infected RAW264.7 cells. PCV2-infected macrophages were treated with FNB, and oxidative stress markers, antioxidant enzyme activities, as well as related gene and protein expression were assessed to evaluate FNB's regulatory effects. Specifically, the level of Nitric Oxide (NO), Total antioxidant capacity (T-AOC), anti-hydroxyl radical capacity, anti-superoxide anion capacity, L-Glutathione (GSH) level, Super Oxide Dismutase (SOD) and Catalase (CAT) were detected. The expression of key oxidative stress-related and signaling pathway genes and proteins was determined by qPCR and western blotting, respectively. The results indicated that FNB reduced intracellular ROS, increased SOD and CAT activities, improved antioxidant capacity, upregulated the mRNA expression levels of *HO-1*, *NQO1*, *Nrf2*, *Pi3kca*, *SOD*, and *HDAC1*, downregulated *AKT*, *Keap1*, and *HAT1*, enhanced HDAC1 activity, and inhibited HAT activity. In conclusion, FNB protects against PCV2-induced oxidative damage by activating the PI3K/AKT pathway and inhibiting Keap1, which collectively enhance the Nrf2/HO-1 antioxidant response.

Keywords FNB, PCV2, Oxidative stress, Molecular mechanism

Porcine circovirus is a single-stranded cyclic DNA virus with an icosahedral capsid structure and is the smallest animal virus¹. To date, only four serotypes have been identified: PCV1, PCV2, PCV3, and PCV4². Notably, PCV2 is a common cause of multi-system failure syndrome (PMWS) in weaned piglets worldwide³, causing huge losses to the pig breeding industry. The pathogenesis of PCV2 may be related to the attack on the body's immune system. PCV2 infection significantly increases the number of macrophages/monocytes in lymphoid tissues in piglets while decreasing the number of immune cells (B cells and T cells), leading to significant lesions in lymphoid tissues and internal organs. Xue⁴ found that inhibiting NFκB activation can reduce the replication efficiency of PCV2 in the host. PCV2 can inhibit apoptosis, increase the survival of infected cells, and promote viral replication by activating the Pi3k/AKT pathway.

An imbalance between the production of free radicals or reactive metabolites, such as ROS, and reactive nitrogen species (RNS) leads to oxidative stress⁵. Viral infection is closely related to oxidative stress, which occurs through various mechanisms, such as by promoting the production of intracellular pro-oxidants and inhibiting the synthesis of antioxidant enzymes, disrupting the balance between oxidative and antioxidant states in cells. Cells can exert some antiviral ability during a viral attack by producing oxidative stress. For instance, Khan⁶ revealed that lung epithelial cells can inhibit the replication of the respiratory syncytial virus (RSV) by increasing intracellular Zn²⁺ levels through oxidative stress. Additionally, oxidative stress generates large amounts of lipid peroxides and free radicals, exacerbating the level of oxidative stress in the body. However, excessive oxidative stress in the body can exacerbate viral attacks on the body⁷. For instance, enterovirus 71 (EV71) can induce high mitochondrial production of ROS, leading to the intracellular replication of the EV71 virus⁸. Besides, Nrf2 regulates oxidative stress and is one of the strongest known antioxidant stress pathways⁹.

¹College of Animal Science and Technology, Guangxi University, Nanning 530005, People's Republic of China. ²Guangxi Academy of Fishery Sciences, Nanning 530021, People's Republic of China. ✉email: panxh@st.gxu.edu.cn; tingjunhu@gxu.edu.cn

Nrf2/HO-1 pathway can exert anti-oxidative stress effects through various pathways, including antioxidant, anti-inflammatory, and reduction of mitochondrial damage. Karna¹⁰ showed that MOTILIPERM extract can activate Nrf2/HO-1 signaling pathway in SD rat testes, thus alleviating oxidative stress damage and improving testicular dysfunction caused by immobilization stress in SD rats. Meanwhile, the Nrf2/HO-1 signaling pathway can exert certain antiviral efficacy, affecting virus replication in cells by alleviating oxidative stress damage induced by viral infection¹¹. ROS are intracellular oxygen-containing chemically reactive chemicals, including superoxide anion, hydroxyl radicals, and hydrogen peroxide. Various viruses can increase ROS levels in infected host cells. RNS are intracellular nitrogen-containing chemically reactive chemicals, including nitric oxide, peroxy nitrite, and nitrogen dioxide. Elevated levels of ROS and RNS lead to oxidative stress and cellular damage. Many studies have shown that PCV2 induces a large accumulation of intracellular ROS^{12–14}. Interestingly, a previous research found that PCV2 infection in 3D4/2 cells can induce the production of a large amount of ROS, activating the NF- κ B and p38/MAPK signaling pathways, thus inhibiting the activation of the antioxidant element Nrf2 to induce oxidative stress¹⁵.

The *Polygonum Indicum* is derived from the whole grass of *Polygonum flaccid Meism* and *Polygonum hydropiper L.* The grasses have three main active ingredients, including flavonoid components, volatile components, and tannins¹⁶. Flavonoids are the main metabolites of *Polygonum hydropiper L.*, including flavones, isoflavones, and flavonoid glycosides. Tao¹⁷ identified the components of FNB, including rutin, quercitrin, and quercetin, via high-performance liquid chromatography high chromatography. Plant flavonoids have powerful antioxidant effects compared with Vitamin C (VC). Zhang discovered that the flavonoids in *Paeonia lactiflora* can effectively scavenge many free radicals, including $O_2^{\cdot-}$, $OH^{\cdot-}$, 1,1-Diphenyl-2-picrylhydrazyl Free Radical (DPPH) and 2, 2'-azino-bis (3-ethylbenzothiazoline-6-sulfonic acid) (ABTS)¹⁸. Lapshina¹⁹ showed that Cranberry flavonoids can effectively scavenge NO, $O_2^{\cdot-}$ and $OH^{\cdot-}$ in vitro. The flavonoids in organisms can also enhance the antioxidant capacity by activating the expression of antioxidant enzyme genes and elevating the activity of antioxidant enzymes in the body, except for directly scavenging free radicals. Olayinka²⁰ found that quercetin can elevate the activity of CAT, SOD, and glutathione S-transferase (GST) in the liver of mice, thus alleviating pro-Carbazine-induced oxidative damage. In addition, flavonoids can exert antioxidant effects by affecting Keap1-Nrf2 binding and promoting the nucleation of Nrf2²¹. The Pi3k/AKT pathway is closely related to oxidative stress and plays an important role in scavenging intracellular ROS²². High ROS levels can decrease Pi3k and AKT phosphorylation levels. Antioxidants can scavenge excess ROS by affecting the intracellular Pi3k/AKT signaling pathway in cells. Dong et al.²³ found that honeysuckle flavonoids can reduce oxidative stress damage induced by the hydrogen peroxide in human umbilical vein endothelial cells (HUVEC) through the Pi3k/Akt/eNOS signaling pathway, indicating that flavonoids can activate this signaling pathway. In addition, previous studies have shown that flavonoids also possess certain antiviral effects. For example, flavones and isoflavones can reduce the activity of avian myeloblastosis virus (AMV) reverse transcriptase²⁴. Flavonoid compounds such as baicalin, quercetin, and kaempferol can inhibit viral adsorption to cells and exhibit good antiviral efficacy in the early stages of viral infection, a function that may be achieved by flavonoids altering cell membrane fluidity²⁵. Quercetin (QUE) can downregulate cellular histone acetylation levels while simultaneously inhibiting the NF- κ B inflammatory signaling pathway and activating the Nrf2/HO-1 antioxidant signaling pathway, thus modulating the production of inflammatory and antioxidant factors, exerting anti-inflammatory and antioxidant effects, and thereby regulating PCV2-induced oxidative stress¹⁵. RAW264.7 cells are a murine macrophage-like cell line that has been widely used in studies of immune responses and viral infections, owing to well-established experimental methods and abundant comparable data. They exhibit typical macrophage functions, closely mimic key aspects of the natural immune response in vivo, are sensitive to viral infection, and are capable of recreating immune responses observed during pathogen invasion in the body. In addition, Chen showed that PCV2 was able to infect RAW264.7 cells²⁶. This study aimed to investigate the molecular mechanism of oxidative stress induced by PCV2 infection in immune cells and explore the protective effect of FNB against PCV2 infection. Therefore, the findings may provide a new idea for the prevention and treatment of PCV2-infected diseases.

Results

Determination of safe FNB concentration on RAW264.7 cells

To investigate the potential inhibitory effect of FNB against PCV2, this study aimed to screen its safe and effective concentration range. Given that macrophages are key target cells for PCV2 during natural infection, the murine macrophage cell line RAW264.7 was selected as the in vitro model for this research. Firstly, the safe concentrations of FNB were determined via a cytotoxicity assay. The results revealed that high concentrations of FNB ($\geq 150 \mu\text{g/mL}$) significantly inhibited cell viability, whereas concentrations of 25, 50, and 75 $\mu\text{g/mL}$ were non-toxic and were therefore selected as the working concentrations for subsequent experiments (Fig. 1A). The protective effects of these three concentrations were evaluated in a PCV2 infection model. The data showed that PCV2 infection markedly reduced the viability of RAW264.7 cells. However, pretreatment with all three selected concentrations of FNB significantly reversed this virus-induced cellular damage ($p < 0.01$) (Fig. 1B). In summary, FNB, at non-cytotoxic concentrations, exhibits significant in vitro protective activity against macrophage damage induced by PCV2 infection. This suggests that FNB holds potential and warrants further investigation for the prevention and treatment of PCV2-associated diseases.

DPPH radical scavenging activity of FNB

The in vitro antioxidant activity of FNB was evaluated using the DPPH radical scavenging assay. As shown in Fig. 2, the scavenging rate of FNB on DPPH radicals increased significantly with concentration in the range of 25–75 $\mu\text{g/mL}$, exhibiting a clear concentration-dependent manner. Although the scavenging activity of FNB was lower than that of the positive control, Vitamin C (Vc), this result indicates that FNB possesses direct antioxidant capacity.

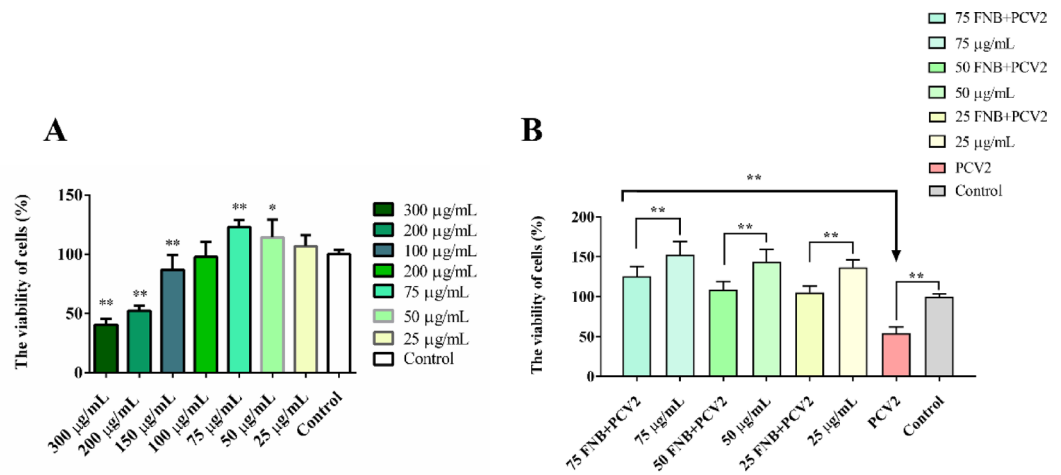


Fig. 1. The viability of RAW264.7 cells (%), $n = 6$. *Notes:* 300 µg/mL: 300 µg/mL FNB; 200 µg/mL: 200 µg/mL FNB; 150 µg/mL: 150 µg/mL FNB; 100 µg/mL: 100 µg/mL FNB; 75 µg/mL: 75 µg/mL FNB; 50 µg/mL: 50 µg/mL FNB; 25 µg/mL: 25 µg/mL FNB; Control: Control group. PCV2: PCV2 infection group. ** $p < 0.01$, * $p < 0.05$.

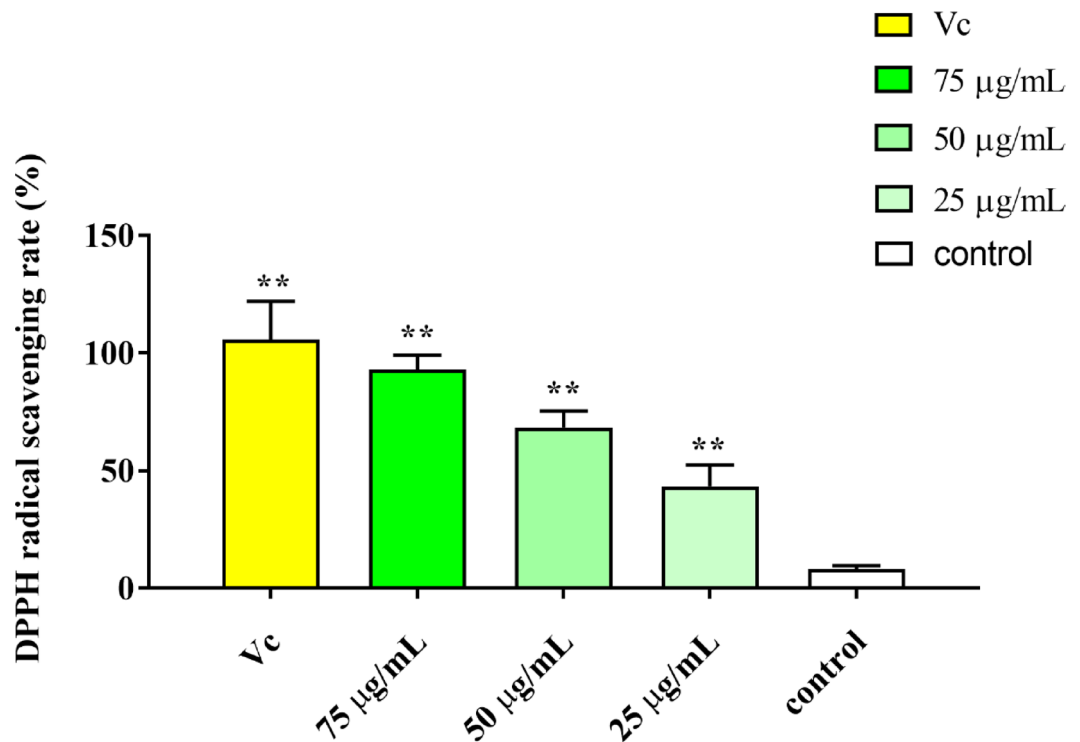


Fig. 2. DPPH Radical Scavenging Activity of FNB (%), $n = 6$. *Notes:* 75 µg/mL: 75 µg/mL FNB; 50 µg/mL: 50 µg/mL FNB; 25 µg/mL: 25 µg/mL FNB; Control: Control group. Vc: VC positive control group. ** $p < 0.01$.

FNB effect on oxidative stress in PCV2-infected RAW264.7 cells

To investigate whether FNB exerts its antiviral activity by modulating cellular oxidative stress, this study measured the intracellular levels of key oxidative stress molecules, namely reactive oxygen species (ROS) and nitric oxide (NO). The results, as depicted in Fig. 3A, B, showed that PCV2 infection significantly upregulated the production of ROS and NO in RAW264.7 cells after 24 h compared to the control group ($p < 0.05$ or $p < 0.01$). In contrast, treatment with FNB (25, 50, and 75 µg/mL) or the positive control Vc significantly suppressed the elevated levels of ROS and NO in PCV2-infected cells ($p < 0.01$). These findings demonstrate that FNB can effectively alleviate oxidative stress by reducing the intracellular levels of ROS and NO induced by viral infection.

To further evaluate the effect of FNB on the overall cellular antioxidant status, this study measured the Total Antioxidant Capacity (T-AOC), as well as the scavenging capacities for superoxide anions and hydroxyl radicals. These parameters collectively reflect the comprehensive defense level of the non-enzymatic antioxidant system.

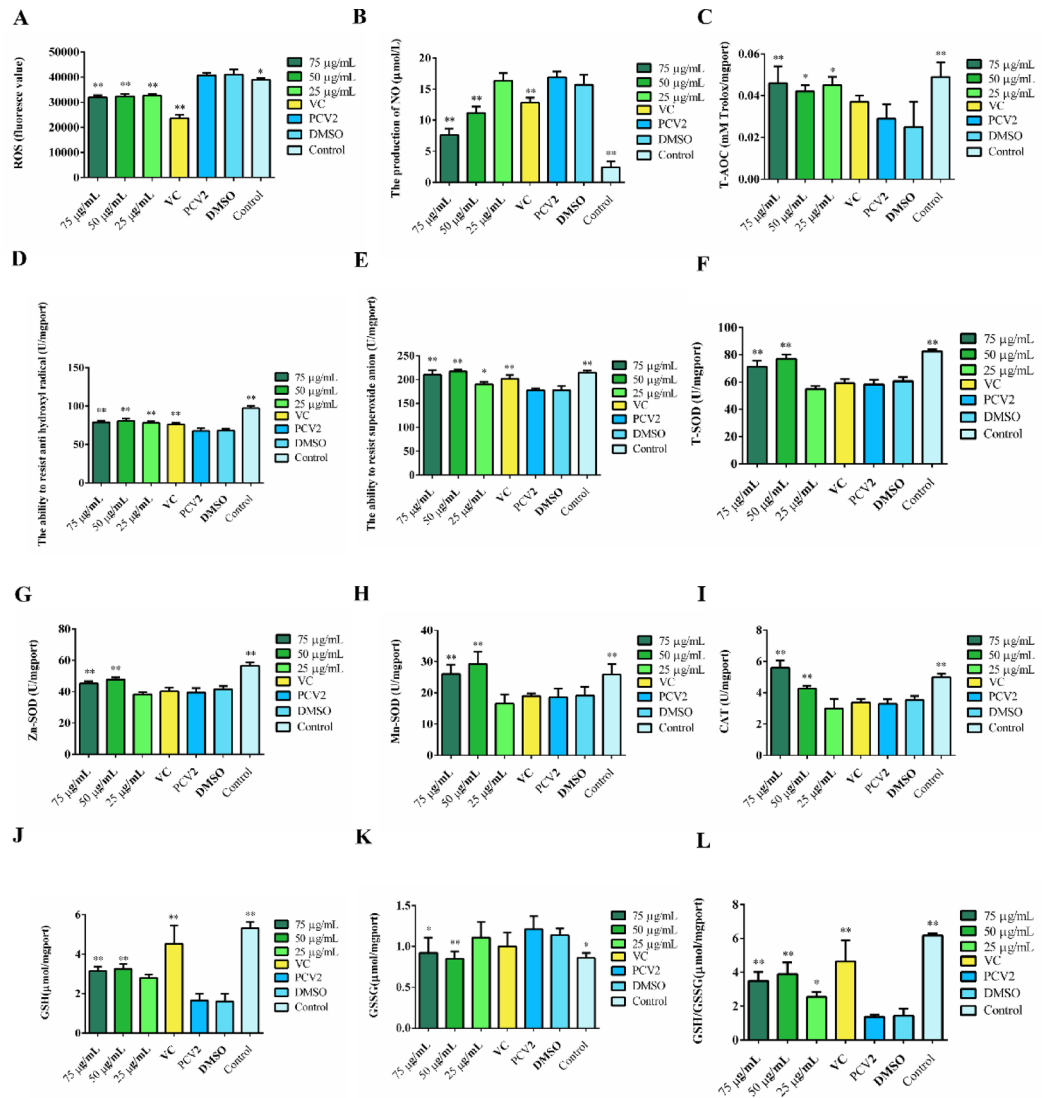


Fig. 3. The effects of FNB on oxidative stress in PCV2-infected RAW264.7 cells. *Notes:* (A) The content of ROS. (B) The content of NO. (C) The content of T-AOC. (D) The intracellular anti-hydroxyl radical activities. (E) The anti-superoxide anion activities. (F) The content of T-SOD. (G) The content of Zn-SOD. (H) The content of Mn-SOD. (I) The content of CAT. (J) The content of GSH. (K) The content of GSSG. (L) The content of GSH/GSSG. 75 µg/mL: 75 µg/mL FNB; 50 µg/mL: 50 µg/mL FNB; 25 µg/mL: 25 µg/mL FNB; VC: VC control group; PCV2: PCV2 infection group; DMSO: RPMII-1640 with 0.05% DMSO; Control: Control group. ** $p < 0.01$; * $p < 0.05$.

As shown in Fig. 3C–E, PCV2 infection significantly diminished the T-AOC, superoxide anion scavenging capacity, and hydroxyl radical scavenging capacity of RAW264.7 cells ($p < 0.01$). Conversely, treatment with FNB at 25, 50, and 75 µg/mL significantly elevated the T-AOC in infected cells ($p < 0.05$ or $p < 0.01$). Furthermore, 25 µg/mL of FNB also significantly enhanced the scavenging efficacy for superoxide anions ($p < 0.05$) and hydroxyl radicals ($p < 0.01$). Similar results were observed for the positive control (VC), whereas the vehicle control (DMSO) exerted no significant effect ($p > 0.05$). Taken together, these data indicate that FNB counteracts viral-induced oxidative damage by bolstering the cell's non-specific total antioxidant capacity, particularly its efficacy in scavenging key free radicals.

To assess the effect of FNB on the endogenous enzymatic antioxidant system, this study measured the activities of key antioxidant enzymes: superoxide dismutase (SOD) and catalase (CAT). Specifically, the analysis of SOD isoforms—cytosolic Cu-ZnSOD and mitochondrial MnSOD—allows for a more precise localization of FNB's protective effects. As illustrated in Fig. 3F–L, PCV2 infection significantly inhibited the activities of total SOD, Cu-ZnSOD, MnSOD, and CAT in RAW264.7 cells ($p < 0.01$). However, pretreatment with FNB at 50 and 75 µg/mL significantly restored the activities of these suppressed enzymes ($p < 0.01$), while the vehicle control (DMSO) did not exert a significant effect ($p > 0.05$). These findings indicate that FNB strengthens the

cellular enzymatic antioxidant defense system, particularly by boosting the activities of SOD and CAT in both the cytosol and mitochondria, thereby counteracting the oxidative stress induced by viral infection.

Glutathione (GSH) is the principal non-enzymatic antioxidant within cells. The ratio of its reduced form (GSH) to its oxidized form (glutathione disulfide, GSSG). The GSH/GSSG ratio, is a critical determinant of the cellular redox state and the degree of oxidative stress. The results revealed that PCV2 infection led to a significant depletion of intracellular GSH content ($p < 0.01$) and severely disrupted the GSH/GSSG ratio ($p < 0.01$) in RAW264.7 cells, indicating a severe redox imbalance (Fig. 3E–G). In comparison, FNB (25–75 $\mu\text{g}/\text{mL}$), as well as the positive control V_c , significantly increased GSH content ($p < 0.01$). Furthermore, FNB treatment (25–75 $\mu\text{g}/\text{mL}$) also reduced GSSG levels ($p < 0.05$ or $p < 0.01$). Crucially, both FNB and V_c treatments significantly restored the GSH/GSSG ratio ($p < 0.01$ or $p < 0.05$), whereas the DMSO control had no significant impact. Collectively, these data provide strong evidence that FNB replenishes the cellular GSH pool, likely by promoting GSH generation and facilitating GSSG recycling, thereby restoring the critical GSH/GSSG balance and maintaining cellular redox homeostasis.

In summary, PCV2 infection induced significant oxidative stress in RAW264.7 cells. This was characterized by a sharp increase in the levels of reactive oxygen species (ROS) and nitric oxide (NO), alongside a significant decrease in total antioxidant capacity (T-AOC), the activities of key antioxidant enzymes (such as SOD and CAT), and the levels of the core non-enzymatic antioxidant GSH, including the critical GSH/GSSG ratio. These results indicate that the endogenous antioxidant defense system was severely compromised. However, treatment with FNB effectively reversed these PCV2-induced pathological changes. FNB not only significantly reduced the levels of ROS and NO but also restored T-AOC and the activities of SOD and CAT, replenished GSH content, and re-established GSH/GSSG homeostasis. Collectively, these findings demonstrate that FNB exerts its potent protective effects via a dual mechanism 1: by directly or indirectly scavenging excessive reactive species, and 2 by repairing and bolstering the cell's endogenous enzymatic and non-enzymatic antioxidant defense systems, thereby effectively alleviating PCV2-induced oxidative damage.

Effect of FNB on mRNA expression of oxidative stress-related genes in PCV2-infected RAW264.7 cells

To elucidate the molecular mechanism by which FNB enhances cellular antioxidant capacity, we evaluated key signaling pathways at the transcriptional level. The results showed that PCV2 infection significantly suppressed the endogenous antioxidant defense system (Fig. 4A–H). Specifically, PCV2 led to a significant downregulation in the mRNA expression levels of key genes in the PI3K/Nrf2 signaling axis (Pi3kca, Nrf2) and their downstream antioxidant target genes (SOD, NQO-1) ($p < 0.05$ or $p < 0.01$). Concurrently, the transcription of the pro-oxidant gene iNOS and the signaling molecule Akt was significantly upregulated ($p < 0.05$ or $p < 0.01$), collectively revealing a strategy by which PCV2 compromises cellular antioxidant defenses at the genetic level. Conversely, FNB treatment (25–75 $\mu\text{g}/\text{mL}$) effectively counteracted the suppressive effects of PCV2. FNB not only significantly upregulated the mRNA expression of Pi3kca, Nrf2, and their downstream antioxidant genes (SOD, NQO-1, HO-1) ($p < 0.05$ or $p < 0.01$), but also concurrently inhibited the overexpression of iNOS and Akt ($p < 0.01$). These data suggest that the core antioxidant mechanism of FNB lies in its ability to effectively activate the PI3K/Akt/Nrf2 signaling pathway. By upregulating the gene transcription of key nodes in this pathway, FNB systematically enhances the expression of the endogenous antioxidant gene cluster, thereby reconstructing the cellular antioxidant defense system to combat PCV2-induced oxidative damage.

Effect of FNB on histone acetylation in PCV2-infected RAW264.7 cells

To investigate whether the regulation of gene expression by FNB involves epigenetic mechanisms, we further assessed its impact on histone acetylation. Our findings indicate that PCV2 infection significantly disrupted histone acetylation homeostasis in RAW264.7 cells (Fig. 5). Although PCV2 concurrently upregulated the activities of both histone acetyltransferases (HATs) and histone deacetylases (HDAC1s), as well as the expression of their related genes (HAT1, HDAC1) ($p < 0.01$), the net effect was a significant increase in the acetylation levels of key histones H3 and H4 ($p < 0.01$). This suggests that PCV2 induces a state of “histone hyperacetylation”, likely to maintain an open chromatin conformation, thereby facilitating the transcription of viral genes and host pro-inflammatory genes like iNOS. However, FNB treatment demonstrated potent epigenetic remodeling capabilities. By significantly inhibiting HAT activity and HAT1 gene expression ($p < 0.01$) while simultaneously enhancing HDAC1 activity, FNB synergistically and robustly reversed the PCV2-induced histone hyperacetylation, leading to a significant decrease in the acetylation levels of both H3 and H4 ($p < 0.01$). These results reveal for the first time that FNB acts not only as an antioxidant but also as a potent epigenetic modulator. By remodeling the cellular acetylating enzyme system, FNB promotes a transcriptionally repressive chromatin state, which may represent a key upstream mechanism underlying its inhibition of viral replication and inflammation.

Effect of FNB on Pi3k/AKT signaling pathway and Nrf2/HO-1 signaling pathway

To confirm whether FNB activation of Nrf2 directly depends on the upstream PI3K/Akt signaling pathway, the specific PI3K inhibitor LY294002 has no toxic effect on RAW264.7 cells and can be used in experiments (Fig. 6A). Western Blot analysis revealed that FNB treatment significantly upregulated the expression of Nrf2 and its target protein HO-1, while concurrently promoting PI3K protein expression and Akt phosphorylation ($p < 0.05$) (Fig. 6B–H). This indicates that FNB can activate the PI3K/Akt/Nrf2 signaling axis. Critically, when cells were pretreated with LY294002 to specifically block the PI3K/Akt pathway, the FNB-induced phosphorylation of Akt was completely inhibited. More importantly, under this condition, the ability of FNB to activate Nrf2 and HO-1 protein expression was also completely abolished ($p > 0.05$). This result provides compelling evidence that the PI3K/Akt pathway plays an indispensable upstream regulatory role in the FNB-mediated activation of Nrf2.

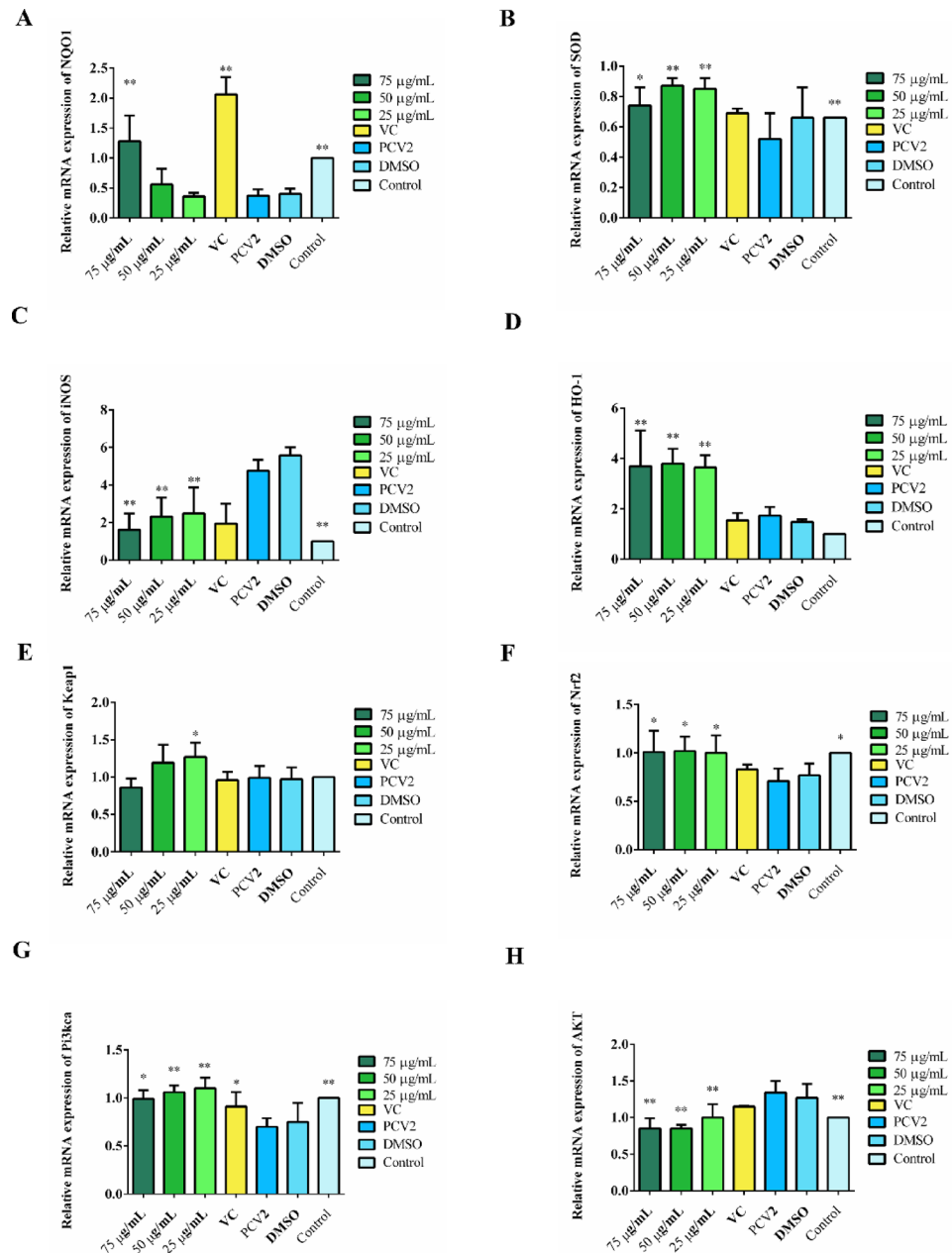


Fig. 4. The mRNA expression level of oxidative stress-related genes. *Notes:* (A) The mRNA expression level of NQO1. (B) The mRNA expression level of SOD. (C) The mRNA expression level of iNOS. (D) The mRNA expression level of HO-1. (E) The mRNA expression level of Keap1. (F) The mRNA expression level of Nrf2. (G) The mRNA expression level of Pi3kca. (H) The mRNA expression level of AKT. 75 µg/mL: 75 µg/mL FNB; 50 µg/mL: 50 µg/mL FNB; 25 µg/mL: 25 µg/mL FNB; VC: VC control group; PCV2: PCV2 infection group; DMSO: RPMII-1640 with 0.05% DMSO; Control: Control group. ** $p < 0.01$; * $p < 0.05$.

Therefore, we conclude that FNB exerts its cytoprotective effects by activating the PI3K/Akt signal cascade, which in turn promotes the activation of the downstream Nrf2/HO-1 pathway.

Effect of FNB on protein expression of Pi3k/AKT and Nrf2/HO-1-related pathways in PCV2-infected RAW264.7 cells

Building on our previous finding that FNB activates Nrf2 via the PI3K/Akt pathway, this study aimed to validate this mechanism in the context of PCV2 infection. We found that while PCV2 infection itself did not significantly alter the activity of the PI3K/Akt pathway ($p > 0.05$), it suppressed the expression of Nrf2 and its downstream target HO-1 by significantly upregulating the Nrf2 negative regulator, Keap1 ($p < 0.05$) (Fig. 7E–H). This reveals a key strategy employed by PCV2 to inhibit the host cell's antioxidant capacity. Against this backdrop, FNB treatment exhibited a potent protective effect. On one hand, FNB effectively reversed the PCV2-

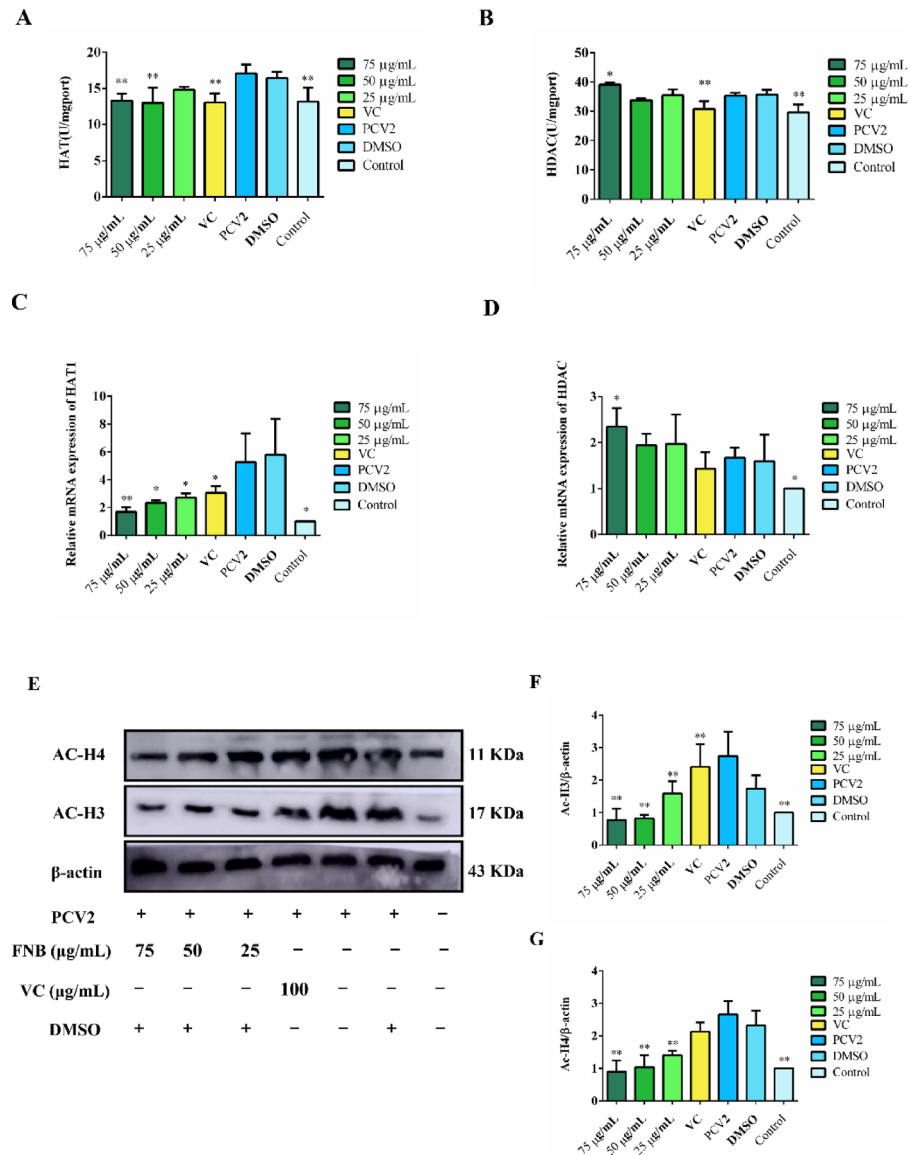


Fig. 5. The effect of FNB on histone acetylation in PCV2-infected RAW264.7 cells. *Notes:* (A) The enzyme activity of HAT. (B) The enzyme activity of HDAC1. (C) The mRNA expression level of HAT1. (D) The mRNA expression level of HDAC1. (E–G) The expression level of AcH3 and AcH4. 75 µg/mL: 75 µg/mL FNB; 50 µg/mL: 50 µg/mL FNB; 25 µg/mL: 25 µg/mL FNB; VC: VC control group; PCV2: PCV2 infection group; DMSO: RPMII-1640 with 0.05% DMSO; Control: Control group. ** $p < 0.01$; * $p < 0.05$.

induced overexpression of Keap1 ($p < 0.05$). On the other hand, it independently and significantly activated the upstream PI3K/Akt signaling pathway, as evidenced by the marked upregulation of both Pi3k-p85 and Akt phosphorylation ($p < 0.01$) (Fig. 7A–D). It is through this dual mechanism—inhibiting Keap1 while activating PI3K/Akt—that FNB synergistically rescued Nrf2 from the viral suppressive effect, ultimately restoring the activity of the Nrf2/HO-1 antioxidant pathway. Therefore, this study confirms that FNB employs a sophisticated dual-track strategy to efficiently activate the Nrf2 pathway in a viral infection model, thereby rebuilding the cellular antioxidant defense line.

Discussion

PCV2 is associated with the multi-system failure syndrome in weaned piglets, seriously affecting the economic efficiency of the pig breeding industry. The continuous PCV2 mutation limits conventional vaccine immunization, necessitating a new, safe, and effective method for PCV2 treatment. *Polygonum officinale*, a traditional herb in China, has anti-inflammatory, anti-oxidative, and immunity-enhancing biological activities. Several studies have shown that PCV2 particles can be detected in lymphoid tissues and immune cells of morbid pigs or dead pigs, suggesting that the pathogenesis of PCV2 is related to the virus attacking the immune system.

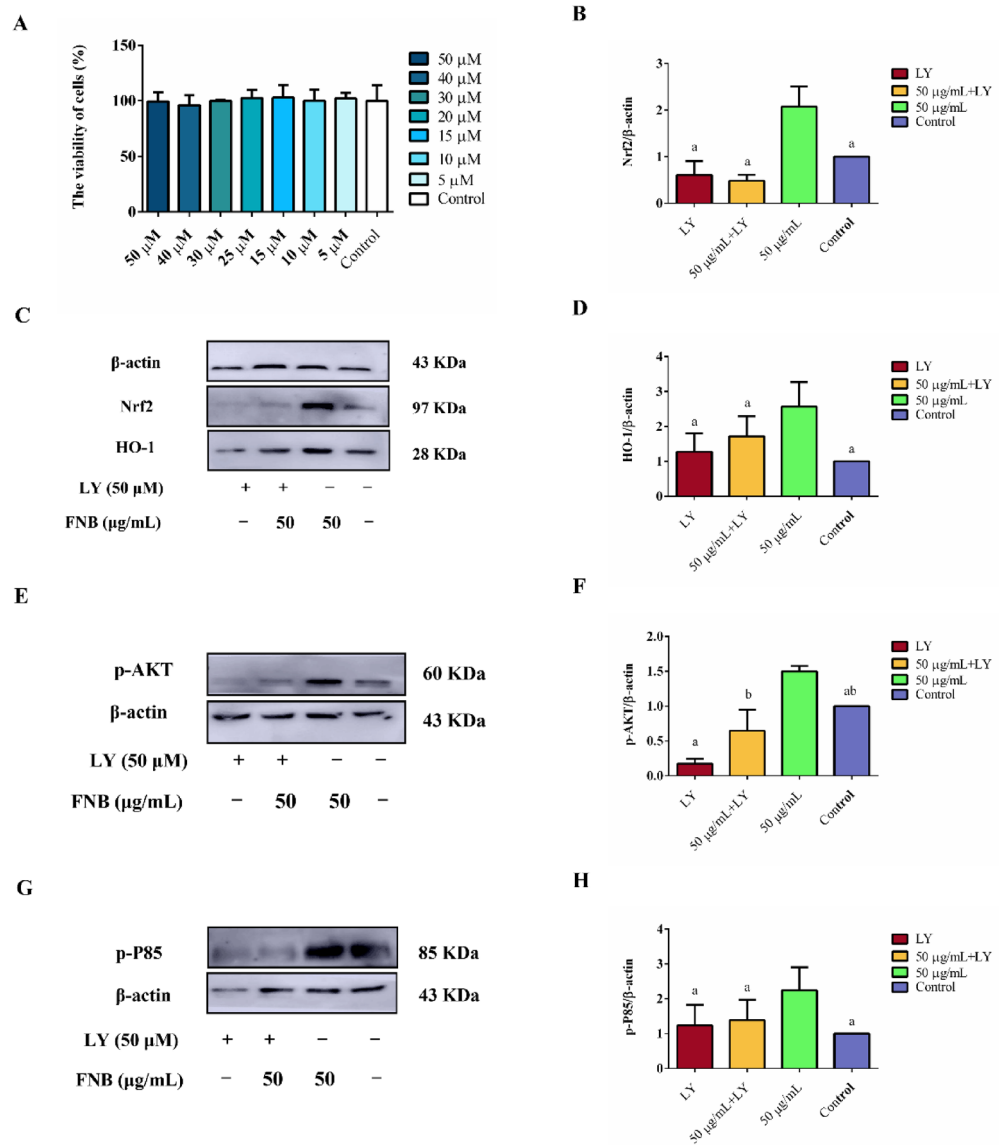


Fig. 6. Effect of FNB on Pi3k/AKT signaling pathway and Nrf2/HO-1 signaling pathway. *Notes:* (A) The effect of LY294002 on the activity of RAW264.7 cells. (B–D) The protein expression level of Nrf2 and HO-1. (E, F) The protein expression level of p-AKT. (G, H) The protein expression level of p-P85. LY:50 μ M LY294002; 50 μ g/mL + LY: 50 μ g/mL FNB + LY294002; 50 μ g/mL: 50 μ g/mL FNB; Control: Control group. the same letter on the shoulder indicates that the difference between groups is not significant ($p > 0.05$), and different letters on the shoulder indicate that the difference between groups is significant ($p < 0.05$).

Various viruses can increase ROS levels in infected host cells. RNS are intracellular nitrogen-containing chemicals and mainly include nitric oxide, peroxynitrite, and nitrogen dioxide. Increased ROS and RNS cause oxidative stress, which can damage cells. Besides, the hepatitis B virus (HBV) can decrease intracellular Cu/Zn-SOD and GPx, causing cellular lipid peroxidation and DNA damage²⁷. In this study, PCV2 infection decreased the anti-hydroxyl radical and superoxide anion capacity of RAW264.7 cells and increased ROS content and NO in RAW264.7 cells, suggesting that PCV2 infection can lead to oxidative stress in RAW264.7 cells. Additionally, flavonoids have anti-oxidative effects and can alleviate the effect of oxidative stress caused by viral infection. Raju²⁸ found that influenza virus infection can significantly increase the level of lipid peroxidation in mice, while quercetin can significantly decrease the level of lipid peroxidation in mice. Herein, FNB significantly reduced the production of ROS and NO in PCV2-infected RAW264.7 cells and improved resistance to hydroxyl radicals, superoxide anions, and anti-oxidative capacity, indicating that FNB has a modulating effect on PCV2-induced oxidative stress.

In this study, the DPPH radical scavenging assay confirmed that FNB possesses direct, concentration-dependent antioxidant activity in vitro. This intrinsic capacity to directly neutralize free radicals serves as a crucial foundation for its cytoprotective effects. Under pathological conditions such as viral infection, cells generate an excess of reactive oxygen species (ROS), leading to oxidative stress. This stress primarily depletes

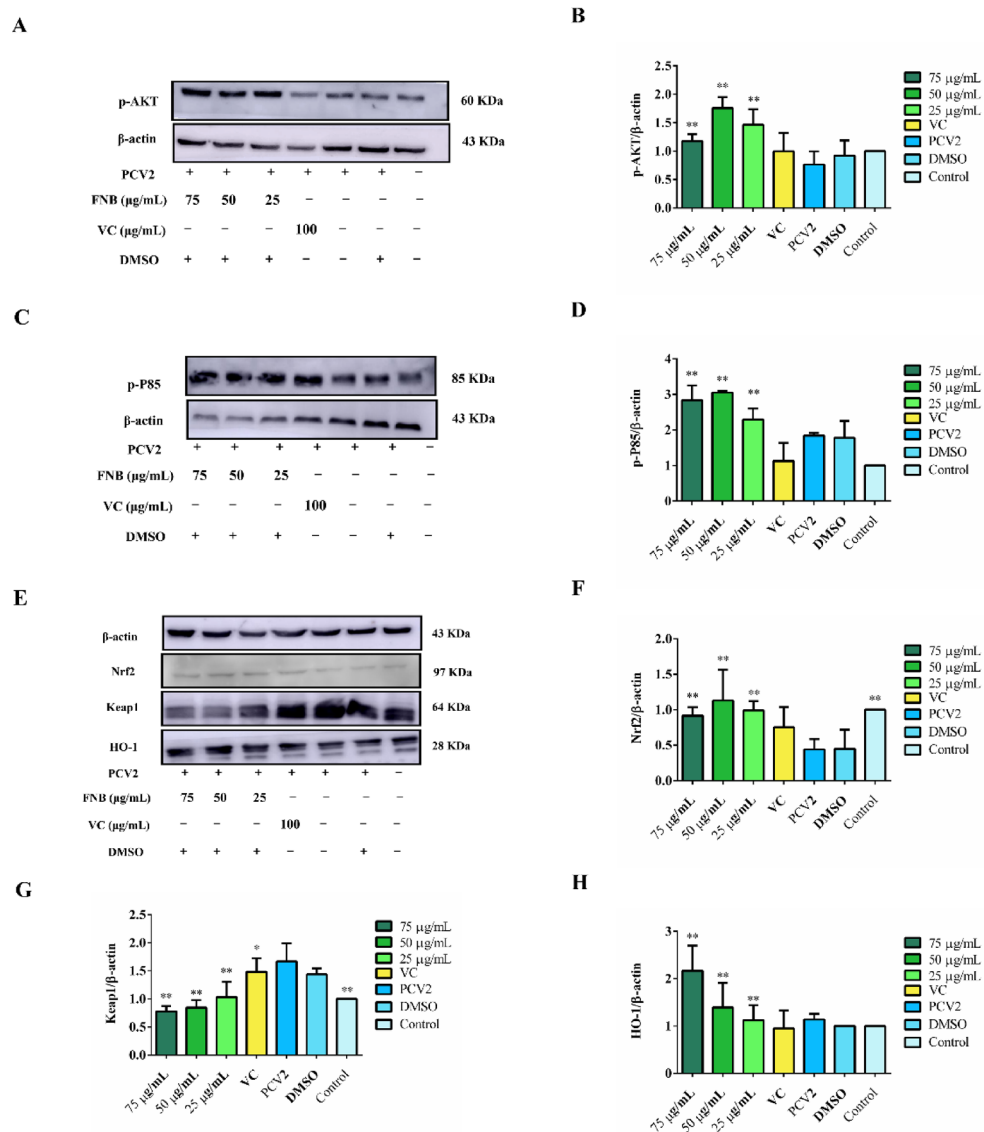


Fig. 7. The effect of FNB on expression levels of proteins associated with Pi3k/AKT and Nrf2/HO-1 pathways in PCV2-infected RAW264.7 cells. *Notes:* (A, B) The protein expression level of p-AKT. (C, D) The protein expression level of p-P85. (E–H) The protein expression level of Nrf2, Keap1, and HO-1. 75 μg/mL: 75 μg/mL FNB; 50 μg/mL: 50 μg/mL FNB; 25 μg/mL: 25 μg/mL FNB; VC: VC control group; PCV2: PCV2 infection group; DMSO: RPMII-1640 with 0.05% DMSO; Control: Control group. ** $p < 0.01$; * $p < 0.05$.

the cell's major non-enzymatic antioxidant, reduced glutathione (GSH), by converting it to its oxidized form (GSSG). Consequently, this results in a decrease in total GSH levels and an imbalance in the critical GSH/GSSG ratio^{29,30}, thereby disrupting the cellular reducing microenvironment. We postulate that FNB, as an exogenous antioxidant, can directly scavenge a portion of the intracellular ROS. By doing so, FNB likely alleviates the burden on the endogenous antioxidant system, effectively sparing GSH from depletion. This protective action would help maintain or even restore the intracellular pool of GSH and its dynamic equilibrium with GSSG, thus stabilizing the GSH/GSSG ratio. Furthermore, the endogenous antioxidant enzyme system—comprising superoxide dismutase (SOD), catalase (CAT), and glutathione peroxidase (GPx)—constitutes the primary line of defense against oxidative damage. Persistent ROS attack can not only inhibit the activity of these enzymes but also downregulate their gene expression. Given that FNB can preemptively neutralize ROS, it can effectively lower the substrate load faced by these enzymes. This indirect protection may prevent the inactivation or downregulation of these antioxidant enzymes, thereby potentially promoting the restoration of their protein expression and activity. In conclusion, the direct radical scavenging ability of FNB demonstrated in the DPPH assay is likely the fundamental mechanism underlying its capacity to restore intracellular GSH homeostasis and enhance the expression of antioxidant enzymes. These two effects are complementary and synergistically bolster the cell's overall resilience against oxidative stress.

SOD is an important anti-oxidative enzyme in mammals, and it can be divided into two types: Cu-ZnSOD and MnSOD. Cu-ZnSOD and MnSOD can scavenge ROS and prevent cell damage caused by ROS accumulation. Besides, SOD has a therapeutic effect on viral infections. Hydrogen peroxide is a metabolic waste produced by the oxidative reactions. Also, excessive accumulation of hydrogen peroxide can further increase cellular oxidative stress and cause irreversible damage to cells. CAT can break down hydrogen peroxide, reducing intracellular hydrogen peroxide levels and maintaining intracellular redox homeostasis. Zhang³¹ found that lemon seed flavonoids can increase the activities of total SOD and CAT in mice and increase the gene expression levels of intracellular Cu-ZnSOD and MnSOD. Herein, PCV2 infection decreased the activities of intracellular anti-oxidative enzymes, while FNB significantly increased SOD and CAT activities, indicating that FNB induces anti-oxidative effects by increasing the activities of intracellular anti-oxidative enzymes. The overexpression of *iNOS* genes causes irreversible damage to proteins and nucleic acids in cells³². Therefore, inhibiting the mRNA expression of *iNOS* and reducing the level of intracellular RNS can attenuate oxidative damage in cells. In this study, FNB significantly decreased the over-expression of intracellular *iNOS* caused by PCV2 infection and reduced the production of intracellular RNS, avoiding further oxidative damage in RAW264.7 cells.

The Nrf2-mediated signaling pathway is one of the most important anti-oxidative stress pathways³³. Studies have found that viruses can affect Nrf2 and cause oxidative stress by breaking down the intracellular redox system. Respiratory syncytial virus infection in vitro and in vivo causes oxidative damage by reducing Nrf2-dependent gene transcription of antioxidant enzymes³⁴. In this study, PCV2 decreased the mRNA expression of *Nrf2*, resulting in an imbalance of the cell redox state. Therefore, increasing mRNA expression of *Nrf2* and anti-oxidative stress capacity of cells can prevent cell damage caused by viral attacks. Xiao found that *Eucommia ulmoides* Flavones can increase mRNA expression of *Nrf2* in porcine jejunal epithelial cells. Moreover, anti-oxidative enzymes, such as *HO-1*, *NQO-1*, and *SOD*, are downstream genes of *Nrf2*³⁵. Herein, FNB treatment significantly increased the mRNA expression of *Nrf2*, which was decreased by PCV2 infection. Also, FNB increased the mRNA expression levels of *HO-1*, *NQO-1*, and *SOD*, suggesting that FNB exerts anti-oxidative effects by affecting Nrf2-related signaling pathways.

The regulation of histone acetylation is a critical epigenetic mechanism for controlling the expression of genes involved in redox homeostasis. This process is dynamically balanced by the opposing activities of histone acetyltransferases (HATs), which add acetyl groups to promote transcriptional activation, and histone deacetylases (HDACs), which remove them to induce gene silencing³⁶. Crucially, cellular oxidative stress can disrupt this balance by altering the activity and expression of these enzymes, creating a complex feedback loop that influences cell fate³⁷. In this study, we observed that PCV2 infection led to a state of histone hyperacetylation, characterized by significantly increased acetylation levels of H3 and H4. This was associated with elevated activity of both HATs and HDACs, suggesting a profound disruption of epigenetic regulation by the virus. We posit that this hyperacetylation creates a permissive chromatin environment, facilitating the transcription of not only viral genes but also host pro-inflammatory genes like *iNOS*, thereby exacerbating oxidative stress. Significantly, treatment with FNB potentially counteracted this phenomenon. FNB administration decreased HAT activity while increasing HDAC activity, leading to a marked reduction in H3 and H4 acetylation. This reversal of the hyperacetylated state demonstrates FNB's strong epigenetic modulatory capacity. While this effect evidently represses pro-viral and pro-inflammatory transcription by promoting a more condensed chromatin structure, we propose it also directly contributes to the restoration of redox homeostasis. The deacetylation of histones at the promoter regions of key antioxidant genes, such as *Nrf2* within the *Nrf2*/*HO-1* pathway could enhance their transcriptional repression or activation³⁸. The ability of FNB to modulate HATs/HDACs is reminiscent of certain natural compounds, such as flavonoids and other polyphenols. For instance, the flavonoid quercetin has been reported to inhibit HATs like p300/CBP³⁹. These compounds leverage epigenetic modulation to exert their antioxidant effects. Therefore, our finding that FNB regulates HAT/HDAC activity provides a novel mechanistic insight into its protective role against PCV2. It suggests that FNB acts, at least in part, as an epigenetic regulator to restore cellular redox balance, a function that warrants further investigation to map the specific histone modifications at the promoters of antioxidant genes.

p85 is a regulatory subunit of Pi3k and its phosphorylation decreases Pi3k activity⁴⁰. Studies demonstrated that the Pi3k/AKT signaling pathway regulates viral infection and plays a bidirectional role in viral infection. In the pre-infection stage of the virus, the virus inhibits autophagy of the cells by stimulating Pi3k/AKT signaling pathway to facilitate replication. Furthermore, protein phosphorylation can induce antiviral response and phosphorylation of Pi3k/AKT can activate the host's intrinsic immune genes to exert antiviral efficacy⁴¹. In a previous study, it was found that the porcine reproductive and respiratory syndrome virus (PRRSV) can infect porcine monocyte-derived dendritic cells (Mo-DCs)⁴². The Pi3k/AKT signaling pathway is activated within the first 4 h after virus infection, after which it is decreased after 12 h of infection. Another study showed that PCV2 infection of PK-15 cells transiently activated the phosphorylation of AKT, which reached a maximum after 1 h of infection but returned to normal levels after 8-h of infection⁴³. In this experiment, there was no significant difference in Pi3k/AKT phosphorylation levels after PCV2 infection compared to the control group, which was similar to the results of Wei et al.⁴³. Meng demonstrated that baicalin activated the Nrf2-mediated *HO-1* signaling pathway to suppress oxidative stress and inflammatory response⁴⁴. In this study, PCV2 infection up-regulated the protein expression level of Keap1, Nrf2 accumulation in the cytoplasm. After FNB treatment, the expression level of Keap1 was significantly decreased and this was accompanied by increased Nrf2 content, which prompted Nrf2 to activate the expression of the downstream anti-oxidative gene *HO-1*. Further analysis showed that the Pi3k/AKT pathway activated the Nrf2 pathway⁴⁵. Therefore, activation of the Pi3k/AKT signaling pathway may induce the anti-oxidative effects in an organism. Rajendran found that kaempferol inhibited zearalenone-induced oxidative stress by up-regulating the expression of *NQO-1* and *HO-1* through the Pi3k/AKT/Nrf2 signaling pathway⁴⁶. Several flavonoids can exert anti-oxidative effects by activating Pi3k/AKT and Nrf2/*HO-1* signaling pathways. For example, 7,8-dihydroxyflavone mitigated oxidative stress-induced

cell damage in human keratinocytes through a mechanism involving the Nrf2/HO-1 and Pi3k/AKT signaling pathways⁴⁷. In the present study, we found that FNB up-regulated the phosphorylation level of Pi3k/AKT and protein expression levels of Nrf2 and HO-1 in RAW264.7 cells. Addition of the inhibitor LY294002 attenuated the increase in Pi3k/AKT phosphorylation induced by FNB, and its capacity to up-regulate Nrf2/HO-1 protein expression was also attenuated, suggesting that FNB may act through the Pi3k/AKT signaling pathway to activate the Nrf2/HO-1 signaling pathway and exerting anti-oxidative effects.

Conclusion

Our findings reveal that FNB alleviates PCV2-induced oxidative stress via a dual mechanism: activating the PI3K/AKT pathway and inhibiting Keap1, which collectively enhance the Nrf2/HO-1 antioxidant response. Moreover, the modulation of histone acetylation by FNB highlights its pleiotropy as a pharmacological agent, warranting further investigation into its intricate pharmacological network.

Materials and methods

Reagents

The FNB was extracted by the pharmacology laboratory of the College of Animal Science and Technology at Guangxi University, as described by Tao et al.¹⁷. Fetal bovine serum (FBS) was sourced from VivaCell, (Shanghai, China). RNAiso Plus and HiScript III-RT SuperMix were sourced from TaKaRa (Dalian, China) and Vazyme (Nanjing, China), respectively. 2×RealStar Green Fast Mixture and RPMI 1640 were obtained from Genstar (Beijing, China) and Sangon Biotech (Shanghai, China), respectively. Ultra-sensitive ECL chemiluminescence kit (P10300) and Elisa kit were obtained from New Saimei Biotechnology (Suzhou, China) and Jiubang Biotechnology Co., Ltd (Fujian, China), respectively. The Pi3k inhibitor (LY294002) and dimethyl sulfoxide DMSO were sourced from Solarbio (Beijing, China). Antibodies were sourced from CST (Mass, USA). Cell Counting Kit-8, ROS Assay, and BCA Protein Concentration Assay Kit were obtained from Biyuntian Biotechnology (Shanghai, China). CAT Visible Light Assay, Total Glutathione (T-GSH)/Oxidized Glutathione (GSSG) Assay, Hydroxyl Radical Assay, superoxide dismutase (SOD), inhibition and generation of superoxide anion radical assay and total antioxidant capacity (T-AOC) reagents were sourced from Nanjing Jiancheng Bioengineering Institute (Nanjing, China).

Cells and viruses

RAW264.7 cells were sourced from Procell Life Science & Technology Co., Ltd (Wuhan, China). PCV2 (SH strain, GenBank NO: AY686763) was isolated from the Laboratory of Animal Disease Diagnosis and Immunity, Nanjing Agricultural University, China. The virulence (0.7 pfu/PK-15) was detected after amplification by PK-15 cells, then stored at −80 °C. The experimental method was permitted by the institutional animal ethics committee (GXU2020-009).

Methods

Determination of cell activity by CCK-8 assay

Determination of safe concentration of FNB on RAW264.7 cells First, the RAW264.7 cells (3×10^5 cells/mL) were incubated in 96-well plates (100 μ L per well) in 5% CO₂ at 37 °C for 24 h (Table 1). The supernatant was removed and washed thrice with PBS. RPMI-1640 (containing 10% CCK8) was added and incubated at 37 °C for 1 h away from light. Absorbance of each group was read at 450 nm. Cell activity was calculated as shown below:

$$\text{Cell activity} = (\text{OD of test group} - \text{OD of the blank group}) / (\text{OD of cell control group} - \text{OD of the blank group}) \times 100\%$$

Determination of safe concentration of Pi3k inhibitor (LY294002) RAW264.7 cells (3×10^5 cells/ml) were incubated in 96-well plates (10 μ L per well) in 5% CO₂ at 37 °C for 24 h. LY294002 (50 μ M, 40 μ M, 30 μ M, 25 μ M, 15 μ M, 10 μ M, 5 μ M and 0 (cell control group)) was then added, incubated in 5% CO₂ at 37 °C for 1 h. The supernatant was removed, washed thrice with PBS, then incubated with RPMI-1640 for 24 h. The RPMI-1640 containing 10% CCK8 was added and incubated at 37 °C for 1 h. The absorbance values were read at 450 nm. Cell activity was calculated as shown below:

Groups	Treatments
300 μ g/mL FNB	RPMI-1640 with 300 μ g/mL FNB
200 μ g/mL FNB	RPMI-1640 with 200 μ g/mL FNB
150 μ g/mL FNB	RPMI-1640 with 150 μ g/mL FNB
100 μ g/mL FNB	RPMI-1640 with 100 μ g/mL FNB
75 μ g/mL FNB	RPMI-1640 with 75 μ g/mL FNB
50 μ g/mL FNB	RPMI-1640 with 50 μ g/mL FNB
25 μ g/mL FNB	RPMI-1640 with 25 μ g/mL FNB
Control	RPMI-1640

Table 1. Experimental groups and safety concentration assay for the treatment of FNB on RAW264.7 cell. FNB, Polygonum Officinale flavonoid n-butano.

Cell activity = (OD of test group – OD of the blank group) / (OD of cell control group – OD of the blank group) × 100%.

DPPH free radical scavenging assay

The DPPH radical scavenging activity of the FNB sample was determined spectrophotometrically. Briefly, 2.0 mL of the sample solution (serially diluted in methanol to 0.03125–0.75 mg/mL) was mixed with 2.0 mL of a 0.1 mM DPPH methanolic solution. The mixture was incubated at room temperature for 30 min in the dark, and the absorbance was measured at 517 nm.

Methanol was used in place of the DPPH solution for the sample blank (A_c), and in place of the sample for the control (A_0). Vitamin C was used as a positive control. The scavenging rate was calculated using the formula:

$$\text{Scavenging rate (\%)} = [(A_0 - (A_s - A_c)) / A_0] \times 100\%.$$

Detection of intracellular ROS content using DCFH-DA fluorescent probe

First, RAW264.7 cells (2×10^6 cells/mL) were spread in 12-well plates and incubated in 5% CO₂ at 37 °C for 24 h (Table 2). The cells were then incubated with diluted PCV2 for 2 h, then washed thrice with PBS. RPMI-1640 containing 75 µg/mL, 50 µg/mL, and 25 µg/mL FNB (final concentration of DMSO; 0.05%) in the 12-well plates. DMSO solvent control group, virus-infected group, control group, and VC group were incubated in 5% CO₂ at 37 °C for 24 h. The cells were scraped off with a cell spatula, then 100 µL of the cells were mixed and transferred to a black 96-well plate. The fluorescence values were measured at excitation and emission wavelengths of 488 nm and 525 nm, respectively.

Determination of antioxidant capacity

The supernatant was collected after FNB treatment for 24 h (Table 2), and then the NO content in the cell culture supernatant was measured using the NO one-step assay kit. The cells were collected with PBS, then ultrasonically crushed. Protein concentration was measured with a BCA kit, while the total antioxidant capacity of intracellular substances was measured using a T-AOC kit. The Hydroxyl Radical Assay Kit and Superoxide Anion Radical Assay Kit were used to assess the capacity of intracellular substances to resist hydroxyl radicals and superoxide anions, respectively. In addition, intracellular SOD and CAT activities were measured using SOD/CAT Kits, while intracellular GSH and GSSG contents were assessed using T-GSH/GSSG test Kits.

The enzyme activities of HDAC1 and HAT

The enzyme activities of HDAC1 and HAT were determined using ELISA kit following the manufacturer's instructions. Briefly, the supernatant of each well was discarded (Table 2), then the cells were washed thrice with PBS.

Detection of mRNA expression

mRNA expression was detected via qPCR. Briefly, the cell culture supernatant was removed (Table 2), then the cells were washed thrice with PBS. Trizol (1 mL) was added to each well, and the cells were left on ice for 5 min for sufficient lysis. The cell lysate was collected, and the total RNA was determined via Takara RNA extraction kit following the manufacturer's instructions. The extracted total RNA was reverse transcribed as DNA, and mRNA expression levels of oxidative stress-related indicators were detected. β -actin was used as the internal reference gene. The primer sequences are shown in the supplementary material.

Detection of protein expression level

Protein expression levels were detected using western blot. Briefly, the cell culture supernatant was removed (Table 2), then the total cell protein was extracted. Protein concentration was determined using the BCA protein assay kit. The protein samples were then transferred to the PVDF membrane after SDS-PAGE electrophoresis, blocked with 5% skimmed milk for 1.5 h, and incubated with a primary antibody at 4 °C overnight. The PVDF membrane was washed thrice using 1 × TBST, then incubated with a secondary antibody for 1.5 h. The PVDF membrane was then reacted with ECL chromogenic solution for 3 min. Protein bands were observed using a protein imaging system, and their grayscale values were calculated.

The grouping and treatment of the Pi3k inhibitor LY294002 assay are shown in Table 3. The concentration of RAW264.7 cells was adjusted to 2×10^6 cells/mL, and the cells were incubated with 5% CO₂ in 6-well plates at

Groups	Treatment of PCV2	Treatments
75 µg/mL FNB	500 µL PCV2	RPMI-1640 with 75 µg/mL FNB
50 µg/mL FNB	500 µL PCV2	RPMI-1640 with 50 µg/mL FNB
25 µg/mL FNB	500 µL PCV2	RPMI-1640 with 25 µg/mL FNB
VC	500 µL PCV2	RPMI-1640 with 100 µg/mL VC
PCV2 group	500 µL PCV2	RPMI-1640
DMSO group	500 µL PCV2	RPMI-1640 with 0.05% DMSO
Control group	500 µL RPMI-1640	RPMI-1640

Table 2. Grouping and processing of ROS detection. FNB, Polygonum Officinale flavonoid n-butanol; DMSO: dimethyl sulfoxide.

Groups	Treatment of LY294002	Treatment of FNB
LY group	50 μ M LY294002	RPMI-1640
LY + FNB group	50 μ M LY294002	RPMI-1640 with 75 μ g/mL FNB
FNB group	RPMI-1640	RPMI-1640 with 75 μ g/mL FNB
Control group	RPMI-1640	RPMI-1640

Table 3. Grouping and treatment with the Pi3k inhibitor LY294002. LY, Pi3k inhibitor LY294002; FNB, Polygonum Officinale flavonoid n-butanol.

37 °C for 24 h. The cells were divided into the FNB group, FNB + LY group, and LY control group. The cell culture supernatant was removed. Moreover, 1 mL RPMI-1640 containing 50 μ M of LY294002 was added to the LY group and FNB + LY group, and 1 mL RPMI-1640 was added to the control group and FNB group. These groups were incubated with 5% CO at 37 °C for 1 h. The cell culture supernatant was removed, and the plates were washed thrice using PBS. RPMI-1640 containing 75 μ g/mL FNB was added to the FNB group and FNB + LY group, while RPMI-1640 was added to the control group and the LY group.

Data processing and analysis

The data were analyzed by one-way analysis of variance (one-way ANOVA) using SPSS 21.0 statistical software. Duncan method was used to compare between groups. Data were expressed as “mean \pm standard deviation”. Shoulder labels * and ** indicate a significant difference ($p < 0.05$) and very significant difference ($p < 0.01$), respectively. In addition, the same letter on the shoulder indicates that the difference between groups is not significant ($p > 0.05$), while different letters on the shoulder indicate significant differences between groups ($p < 0.05$).

Data availability

All data generated or analysed during this study are included in this published article (and its Supplementary Information files).

Received: 27 June 2024; Accepted: 30 July 2025

Published online: 08 August 2025

References

- Rosario, K. et al. Revisiting the taxonomy of the family Circoviridae: Establishment of the genus Cyclovirus and removal of the genus Gyrovirus. *Arch. Virol.* **162**(5), 1447–1463. <https://doi.org/10.1007/s00705-017-3247-y> (2017).
- Ge, M. et al. Prevalence and genetic analysis of porcine circovirus 3 in China From 2019 to 2020. *Front. Vet. Sci.* **8**, 773912. <https://doi.org/10.3389/fvets.2021.773912> (2021).
- Li, N. et al. Genetic diversity and prevalence of porcine circovirus type 2 in China during 2000–2019. *Front. Vet. Sci.* **8**, 788172. <https://doi.org/10.3389/fvets.2021.788172> (2021).
- Xue, H. et al. Astragalus polysaccharides inhibits PCV2 replication by inhibiting oxidative stress and blocking NF- κ B pathway. *Int. J. Biol. Macromol.* **81**, 22–30. <https://doi.org/10.1016/j.ijbiomac.2015.07.050> (2015).
- Zhuang, C., Wu, Z., Xing, C. & Miao, Z. Small molecules inhibiting Keap1-Nrf2 protein-protein interactions: A novel approach to activate Nrf2 function. *Medchemcomm* **8**(2), 286–294. <https://doi.org/10.1039/c6md00500d> (2016).
- Khan, N. A., Singla, M., Samal, S., Lodha, R. & Medigeshi, G. R. Respiratory syncytial virus-induced oxidative stress leads to an increase in labile zinc pools in lung epithelial cells. *mSphere* **5**(3), e00447–20. <https://doi.org/10.1128/mSphere.00447-20> (2020).
- Liu, D. et al. Selenizing astragalus polysaccharide attenuates PCV2 replication promotion caused by oxidative stress through autophagy inhibition via PI3K/AKT activation. *Int. J. Biol. Macromol.* **108**, 350–359. <https://doi.org/10.1016/j.ijbiomac.2017.12.010> (2018).
- Cheng, M. L., Weng, S. F., Kuo, C. H. & Ho, H. Y. Enterovirus 71 induces mitochondrial reactive oxygen species generation that is required for efficient replication. *PLoS ONE* **9**(11), e113234. <https://doi.org/10.1371/journal.pone.0113234> (2014).
- Chen, B., Lu, Y., Chen, Y. & Cheng, J. The role of Nrf2 in oxidative stress-induced endothelial injuries. *J. Endocrinol.* **225**(3), R83–R99. <https://doi.org/10.1530/JOE-14-0662> (2015).
- Karna, K. K. et al. MOTILIPERM ameliorates immobilization stress-induced testicular dysfunction via inhibition of oxidative stress and modulation of the Nrf2/HO-1 pathway in SD rats. *Int. J. Mol. Sci.* **21**(13), 4750. <https://doi.org/10.3390/ijms21134750> (2020).
- Zhou, J., Zheng, Q. & Chen, Z. The Nrf2 pathway in liver diseases. *Front. Cell Dev. Biol.* **10**, 826204. <https://doi.org/10.3389/fcell.2022.826204> (2022).
- Zhai, N. et al. PCV2 replication promoted by oxidative stress is dependent on the regulation of autophagy on apoptosis. *Vet. Res.* **50**(1), 19. <https://doi.org/10.1186/s13567-019-0637-z> (2019).
- Wang, Q. H. et al. The effect of Panax notoginseng saponins on oxidative stress induced by PCV2 infection in immune cells: In vitro and in vivo studies. *J. Vet. Sci.* **21**(4), e61. <https://doi.org/10.4142/jvs.2020.21.e61> (2020).
- Zhang, Y., Sun, R., Li, X. & Fang, W. Porcine circovirus 2 induction of ROS is responsible for mitophagy in PK-15 cells via activation of Drp1 phosphorylation. *Viruses* **12**(3), 289. <https://doi.org/10.3390/v12030289> (2020).
- Chen, Q. et al. Intervening effects and molecular mechanism of quercitrin on PCV2-induced histone acetylation, oxidative stress and inflammatory response in 3D4/2 cells. *Antioxidants (Basel)* **11**(5), 941. <https://doi.org/10.3390/antiox11050941> (2022).
- Arya, A. K. et al. Ethnomedicinal use, phytochemistry, and other potential application of aquatic and semiaquatic medicinal plants. *Evid. Based Complement. Alternat. Med.* <https://doi.org/10.1155/2022/4931556> (2022).
- Tao, J., Wei, Y. & Hu, T. Flavonoids of *Polygonum hydropiper* L. attenuates lipopolysaccharide-induced inflammatory injury via suppressing phosphorylation in MAPKs pathways. *BMC Complement. Altern. Med.* **16**, 25. <https://doi.org/10.1186/s12906-016-018-8U> (2016).
- Zhang, H. et al. Antioxidant activities and chemical constituents of flavonoids from the flower of *Paeonia ostii*. *Molecules* **22**(1), 5. <https://doi.org/10.3390/molecules22010005> (2016).

19. Lapshina, E. A. et al. Cranberry flavonoids prevent toxic rat liver mitochondrial damage in vivo and scavenge free radicals in vitro. *Cell Biochem. Funct.* **33**(4), 202–210. <https://doi.org/10.1002/cbf.3104> (2015).
20. Olayinka, E. T. et al. Quercetin, a flavonoid antioxidant, ameliorated procarbazine-induced oxidative damage to murine tissues. *Antioxidants (Basel)* **4**(2), 304–321. <https://doi.org/10.3390/antiox4020304> (2015).
21. Jin, Y. et al. Quercetin attenuates toosendanin-induced hepatotoxicity through inducing the Nrf2/GCL/GSH antioxidant signaling pathway. *Acta Pharmacol. Sin.* **40**(1), 75–85. <https://doi.org/10.1038/s41401-018-0024-8> (2019).
22. Yu, J. S. & Cui, W. Proliferation, survival and metabolism: The role of PI3K/AKT/mTOR signalling in pluripotency and cell fate determination. *Development* **143**(17), 3050–3060. <https://doi.org/10.1242/dev.137075> (2016).
23. Dong, J. M. et al. Effects and related mechanism of flavone from *Galium verum* L. on peroxide-induced oxidative injury in human umbilical vein endothelial cells. *Zhonghua Xin Xue Guan Bing Za Zhi* **44**(7), 610–615. <https://doi.org/10.3760/cma.j.issn.0253-3758.2016.07.011E> (2016).
24. Inouye, Y., Yamaguchi, K., Take, Y. & Nakamura, S. Inhibition of avian myeloblastosis virus reverse transcriptase by flavones and isoflavones. *J. Antibiot.* **42**(10), 1523–1525. <https://doi.org/10.7164/antibiotics.42.1523> (1989).
25. Guo, S. S., Shi, Y. J., Gao, Y. J., Su, D. & Cui, X. L. The cytology mechanism of anti-parainfluenza virus infection of total flavone of *Scutellaria barbata*. *Acta Pharmaceutica Sinica* **44**(12), 1348–1352 (2009).
26. Chen, Q. et al. Sophora subprostrate polysaccharide targets LncRNA MSTRG.5823.1 to suppress PCV2-mediated immunosuppression via TNF/NF- κ B signaling. *Int. Immunopharmacol.* **139**, 112701 (2024).
27. Paracha, U. Z. et al. Oxidative stress and hepatitis C virus. *Virol. J.* **10**, 251. <https://doi.org/10.1186/1743-422X-10-251> (2013).
28. Raju, T. A., Lakshmi, A. N., Anand, T., Rao, L. V. & Sharma, G. Protective effects of quercetin during influenza virus-induced oxidative stress. *Asia Pac. J. Clin. Nutr.* **9**(4), 314–317. <https://doi.org/10.1046/j.1440-6047.2000.00162.x> (2000).
29. Wang, Y. et al. Quercetin alleviates acute kidney injury by inhibiting ferroptosis. *J. Adv. Res.* **28**, 231–243. <https://doi.org/10.1016/j.jare.2020.07.007> (2020).
30. Londero, É. P. et al. Rutin-added diet protects silver catfish liver against oxytetracycline-induced oxidative stress and apoptosis. *Comp. Biochem. Physiol. C Toxicol. Pharmacol.* **239**, 108848. <https://doi.org/10.1016/j.cbpc.2020.108848> (2021).
31. Zhang, Y., Li, A. & Yang, X. Effect of lemon seed flavonoids on the anti-fatigue and antioxidant effects of exhausted running exercise mice. *J. Food Biochem.* **45**(4), e13620. <https://doi.org/10.1111/jfbc.13620> (2021).
32. Król, M. & Kepinska, M. Human nitric oxide synthase—its functions, polymorphisms, and inhibitors in the context of inflammation, diabetes and cardiovascular diseases. *Int. J. Mol. Sci.* **22**(1), 56. <https://doi.org/10.3390/ijms22010056> (2020).
33. Qin, S. et al. Phytochemical activators of Nrf2: A review of therapeutic strategies in diabetes. *Acta Biochim. Biophys. Sin. (Shanghai)* **55**(1), 11–22. <https://doi.org/10.3724/abbs.2022192> (2022).
34. Komaravelli, N. et al. Respiratory syncytial virus infection down-regulates antioxidant enzyme expression by triggering deacetylation-proteasomal degradation of Nrf2. *Free Radic. Biol. Med.* **88**(Pt B), 391–403. <https://doi.org/10.1016/j.freeradbiomed.2015.05.043> (2015).
35. Xiao, D. et al. The role of Nrf2 signaling pathway in eucommia ulmoides flavones regulating oxidative stress in the intestine of piglets. *Oxid. Med. Cell Longev.* **2019**, 9719618. <https://doi.org/10.1155/2019/9719618> (2019).
36. Mercado, N. et al. Decreased histone deacetylase 2 impairs Nrf2 activation by oxidative stress. *Biochem. Biophys. Res. Commun.* **406**(2), 292–298. <https://doi.org/10.1016/j.bbrc.2011.02.035> (2011).
37. Vaziri, H. et al. hSIR2(SIRT1) functions as an NAD-dependent p53 deacetylase. *Cell* **107**(2), 149–159. [https://doi.org/10.1016/s0092-8674\(01\)00527-x](https://doi.org/10.1016/s0092-8674(01)00527-x) (2001).
38. Wei, L., Kang, M., Zhang, G., Meng, Y. & Qin, H. (2025) SIRT6 overexpression enhances diabetic foot ulcer healing via Nrf2 pathway activation. *Inflammation* <https://doi.org/10.1007/s10753-025-02297-2> (2025).
39. Xiao, X. et al. Quercetin suppresses cyclooxygenase-2 expression and angiogenesis through inactivation of P300 signaling. *PLoS ONE* **6**(8), e22934. <https://doi.org/10.1371/journal.pone.0022934> (2011).
40. Lee, J. M., Liu, R. & Park, S. W. The regulatory subunits of PI3K, p85 α and p85 β , differentially affect BRD7-mediated regulation of insulin signaling. *J. Mol. Cell Biol.* **13**(12), 889–901. <https://doi.org/10.1093/jmcb/mjab073> (2022).
41. Dunn, E. F. & Connor, J. H. HijAkt: The PI3K/Akt pathway in virus replication and pathogenesis. *Prog. Mol. Biol. Transl. Sci.* **106**, 223–250. <https://doi.org/10.1016/B978-0-12-396456-4.00002X> (2012).
42. Zhang, H. & Wang, X. A dual effect of porcine reproductive and respiratory syndrome virus replication on the phosphatidylinositol-3-kinase-dependent Akt pathway. *Arch. Virol.* **155**(4), 571–575. <https://doi.org/10.1007/s00705-010-0611-6> (2010).
43. Wei, L., Zhu, S., Wang, J. & Liu, J. Activation of the phosphatidylinositol 3-kinase/Akt signaling pathway during porcine circovirus type 2 infection facilitates cell survival and viral replication. *J. Virol.* **86**(24), 13589–13597. <https://doi.org/10.1128/JVI.01697-12> (2012).
44. Meng, X., Hu, L. & Li, W. Baicalin ameliorates lipopolysaccharide-induced acute lung injury in mice by suppressing oxidative stress and inflammation via the activation of the Nrf2-mediated HO-1 signaling pathway. *Naunyn-Schmiedeberg's Arch. Pharmacol.* **392**(11), 1421–1433. <https://doi.org/10.1007/s00210-019-01680-9> (2019).
45. Reddy, N. M. et al. PI3K-AKT signaling via Nrf2 protects against hyperoxia-induced acute lung injury, but promotes inflammation post-injury independent of Nrf2 in mice. *PLoS ONE* **10**(6), e0129676. <https://doi.org/10.1371/journal.pone.0129676> (2015).
46. Rajendran, P. et al. Kaempferol inhibits zearalenone-induced oxidative stress and apoptosis via the PI3K/Akt-mediated Nrf2 signaling pathway: In vitro and in vivo studies. *Int. J. Mol. Sci.* **22**(1), 217. <https://doi.org/10.3390/ijms22010217> (2020).
47. Ryu, M. J. et al. 7,8-Dihydroxyflavone protects human keratinocytes against oxidative stress-induced cell damage via the ERK and PI3K/Akt-mediated Nrf2/HO-1 signaling pathways. *Int. J. Mol. Med.* **33**(4), 964–970. <https://doi.org/10.3892/ijmm.2014.1643> (2014).

Acknowledgements

The authors thank the staff and postgraduate students of the Pharmacology and Toxicology Laboratory of the College of Animal Science and Technology of Guangxi University.

Author contributions

Qi Chen: Conceptualization, methodology, data curation, writing—original draft. Qihua Wang: Data curation, validation, investigation. Yi Zhao: Formal analysis. Xiaodong Xie: Visualization. HeYu Feng: Data curation, software. Yingyi Wei: Resources. Meiling Yu: Supervision. Xianhui Pan: Supervision, investigation. TingJun Hu: Conceptualization, funding acquisition, project administration, supervision, writing—review and editing.

Funding

This work was supported by the [National Natural Science Foundation of China #1] under Grant [Number 32072907]; [Scientific Research and Technology Development Project of Nanning City #2] under Grant [Number 20232039]; [Innovation Project of Guangxi Graduate Education #3] under Grant [Number JGY2023015]; [Innovation and Entrepreneurship Training Program for College Students of Guangxi University #4] under

Grant [Number S202310593294] and [the Project of Bama County for Talents in Science and Technology #5] under Grant [Number 202100182, 20220024].

Declarations

Competing interests

The authors declare no competing interests.

Additional information

Supplementary Information The online version contains supplementary material available at <https://doi.org/10.1038/s41598-025-14362-9>.

Correspondence and requests for materials should be addressed to X.P. or T.H.

Reprints and permissions information is available at www.nature.com/reprints.

Publisher's note Springer Nature remains neutral with regard to jurisdictional claims in published maps and institutional affiliations.

Open Access This article is licensed under a Creative Commons Attribution-NonCommercial-NoDerivatives 4.0 International License, which permits any non-commercial use, sharing, distribution and reproduction in any medium or format, as long as you give appropriate credit to the original author(s) and the source, provide a link to the Creative Commons licence, and indicate if you modified the licensed material. You do not have permission under this licence to share adapted material derived from this article or parts of it. The images or other third party material in this article are included in the article's Creative Commons licence, unless indicated otherwise in a credit line to the material. If material is not included in the article's Creative Commons licence and your intended use is not permitted by statutory regulation or exceeds the permitted use, you will need to obtain permission directly from the copyright holder. To view a copy of this licence, visit <http://creativecommons.org/licenses/by-nc-nd/4.0/>.

© The Author(s) 2025